



## The influence of shaped TiO<sub>2</sub> nanofillers on the thermal properties of poly(vinyl alcohol)

MARIJA B. RADOIČIĆ<sup>1</sup>, ZORAN V. ŠAPONJIĆ<sup>1\*</sup>,  
MILENA T. MARINOVIC-CINCOVIĆ<sup>1</sup>, SCOTT P. AHRENKIEL<sup>2</sup>,  
NATAŠA M. BIBIĆ<sup>1</sup> and JOVAN M. NEDELJKOVIĆ<sup>1</sup>

<sup>1</sup>Vinča Institute of Nuclear Sciences, P.O. Box 522, 11001 Belgrade, Serbia and

<sup>2</sup>South Dakota School of Mines and Technology, Rapid City, SD, USA

(Received 31 March, revised 29 June 2011)

**Abstract:** Poly(vinyl alcohol)-based nanocomposites consisting of shaped TiO<sub>2</sub> nanocrystals (nanoparticles, nanotubes or nanorods) were synthesized by direct blending of the polymer and a solution of titania nanocrystals or powder. In order to elucidate the influence of the shape of the titania nanocrystals on thermal stability of the polymer matrix and particles interaction with poly(vinyl alcohol) (PVA) chains, structural and thermal characterizations of PVA/TiO<sub>2</sub> nanocomposites were performed. Faceted nanoparticles increased the thermal stability of the PVA matrix. Titania nanotubes and nanorods did not show any stabilizing effect on the polymer matrix under an argon atmosphere. The thermo-oxidative degradation temperature of PVA increased with addition of faceted TiO<sub>2</sub> nanoparticles. The thermo-oxidative stability of the PVA matrix was affected more by the presence of titania nanotubes and nanorods in comparison with its thermal stability under an inert atmosphere. The degree crystallinity ( $X_c=32\%$ ) of the PVA matrix slightly decreased in the presence of the faceted TiO<sub>2</sub> nanoparticles in nanocomposite samples.

**Keywords:** nanocomposite materials; thermal properties; differential scanning calorimetry; thermogravimetric analysis; TiO<sub>2</sub>; poly(vinyl alcohol).

### INTRODUCTION

The usage of nanoparticles instead of sub-micron- or micron-sized particles as polymer fillers presents a new dimension in the development and application of this class of advanced materials.<sup>1,2</sup> The main benefits of this type of composite materials are based on the large specific surface area of nanocrystals and their size and shape dependent properties, such as enhanced chemical reactivity and specific bindings. On the other hand, they are based on the desired properties of the polymer matrix, such as long-term stability, reprocessability, etc. Although

\*Corresponding author. E-mail: saponjic@vinca.rs  
doi: 10.2298/JSC110331161R

the individual features of both inorganic and organic constituents of nanocomposite are preserved, their synergy can produce completely novel functionalities. However, the resulting properties of nanocomposites are primarily the simple combination of the properties of all the constituents.

Nanocomposites posses several advantages, such as greater thermal stability, increased strength, enhanced electrical conductivity, improved flammability properties, *etc.* of polymer matrix. Much effort has been made to improve these properties by changing the size and shape as well as amount of applied nanoparticles. However, still not all the possibilities have been completely exploited.<sup>3–5</sup>

The preparation methods of polymer nanocomposites are mainly based on *in situ* polymerization processes in the presence of nanoparticles and direct blending of a polymer solution, a polymer melt or emulsion with solutions of nanoparticles or nanoparticle powders.<sup>6</sup>

Poly(vinyl alcohol) (PVA) is a non-toxic and water-soluble synthetic polymer which has been predominantly utilized for biochemical and medical applications due to its excellent biocompatibility.<sup>7,8</sup> Additionally, owing to its easy processability and optical transparency, semi-crystalline PVA is widely applied as a polymer matrix for the synthesis of nanocomposites by cost efficient and environmentally friendly direct blending methods.<sup>9–11</sup>

Recent achievements in the synthesis of various metal–oxide nanoparticles of different chemical composition, size and shape opened up new possibilities for the preparation and design of polymer/metal oxide nanocomposites. Titanium dioxide ( $\text{TiO}_2$ ) nanoparticles are of particular importance due to their potential applications in different fields, such as photocatalytic degradation of hazardous industrial byproducts or nanocrystalline solar cells.<sup>12,13</sup> X-Ray absorption spectroscopic studies showed that the surface states in  $\text{TiO}_2$  nanocrystallites ( $d < 25$  nm) are characterized by coordinately unsaturated (penta-coordinated) Ti sites formed upon nanoparticle surface reconstruction.<sup>14</sup> The existence of such unique surface structures of  $\text{TiO}_2$  nanoparticles allows control of the surface chemistry in the direction of enhanced coupling of polymer chains and titania nanoparticles.

In this work, the direct blending method was applied for the synthesis of PVA/ $\text{TiO}_2$  nanocomposites using differently shaped titania nanoparticles, such as faceted nanoparticles, nanotubes and nanorods as precursors. The size and shape of applied nanofillers were examined by transmission electron microscopy (TEM). The interaction between oxygen-containing groups within the polymer chains and surface hydroxyl groups of the titania nanoparticles was studied by Fourier transform infrared (FTIR) spectroscopy in the reflection mode. The influence of both the content and shape of the fillers on the overall polymer thermal stability in air and inert atmospheres, as well as the crystallization behavior of the PVA matrix was investigated by non-isothermal thermogravimetry (TGA) and differential scanning calorimetry (DSC) analysis.



## EXPERIMENTAL

*Materials*

All chemicals (PVA ( $M_w = 72,000$  g mol<sup>-1</sup>, hydrolysis degree min. 99 %), TiCl<sub>4</sub> (Merck), H<sub>2</sub>SO<sub>4</sub> (Aldrich) and TiO<sub>2</sub> powder (Fluka) were reagent-grade and used without further purification. Milli-Q deionized water was used as a solvent. Air and argon gases were of high purity (99.5 %). An acid digestion bomb, model 4746 (Parr Instruments), was used for the synthesis of titania nanotubes and nanorods.

*Synthesis of colloidal TiO<sub>2</sub> nanoparticles*

Colloidal TiO<sub>2</sub> nanoparticles were prepared by the controlled hydrolysis of titanium tetrachloride.<sup>15</sup> A solution of TiCl<sub>4</sub>, cooled to -20 °C, was added drop-wise to cold water (at 4 °C) under vigorous stirring and then held at this temperature for 30 min. The pH of the solution was between 0 and 1, depending on the TiCl<sub>4</sub> concentration. Slow growth of the particles was achieved by dialysis against water at 4 °C until the pH of the solution reached 3.5. The final concentration of TiO<sub>2</sub> colloidal solution (0.14 M) was determined from the concentration of the peroxide complex obtained after dissolution of the particles in concentrated H<sub>2</sub>SO<sub>4</sub>.<sup>16</sup>

*Synthesis of TiO<sub>2</sub> nanotubes*

Scrolled titania nanotubes were synthesized by the hydrothermal treatment (20 h/150 °C) of TiO<sub>2</sub> powder (250 mg) dispersed in 10 ml of proton deficient aqueous solution (10 M NaOH) without shaking.<sup>17</sup> After autoclaving, the ensuing powders were sequentially washed with an aqueous 0.1 M HCl solution and distilled water. This washing procedure was repeated until the water reached pH 7. Finally, the powder was separated from the washing solution by centrifugation. The synthesized nanotubes were dried at 70 °C until attainment of a constant mass.

*Synthesis of TiO<sub>2</sub> nanorods*

Rod shaped TiO<sub>2</sub> nanocrystals were prepared from the titania nanotubes in an additional hydrothermal treatment.<sup>18</sup> Dry nanotubes (50 mg) were dispersed in 10 ml of distilled water (pH 7), transferred into a Teflon vessel and treated under saturated vapor pressure of water at 250 °C for 90 min. After autoclaving, the synthesized nanorods were dried at 70 °C to constant mass.

*Synthesis of PVA/TiO<sub>2</sub> nanocomposites*

The PVA/TiO<sub>2</sub> nanocomposites were synthesized from TiO<sub>2</sub> nanoparticles of different shapes and PVA. The polymer (1.5 mass %) was dissolved in boiling water and its concentration was kept constant in all synthesis. The content of THE inorganic phase (TiO<sub>2</sub>) in each nanocomposite sample was 0.25 mass %. Direct mixing of the aqueous PVA solution with an adequate amount of colloidal TiO<sub>2</sub> solution or TiO<sub>2</sub> powder resulted in the formation of a stable and transparent PVA/TiO<sub>2</sub> (particles/tubes/rods) dispersion. The mixture was placed into a Petri dish and dried in a vacuum oven at 40 °C for 24 h. After solvent evaporation, transparent solid films were obtained. A neat PVA film, without the addition of the inorganic phase, was prepared in the same manner.

*Characterization*

The sizes and shapes of the used titania nanoparticles were determined by transmission electron microscopy (TEM) using a JEOL 100CX microscope operating at 100 kV. The morphology of the titania nanotubes was characterized by TEM using a Hitachi H-7000 FA mic-



roscope with a W filament at a high tension of up to 125 kV. The TEM samples were prepared by drop-wise addition of 6 µl of a dispersion of TiO<sub>2</sub> nanoparticles that had been subjected to 10 min of ultrasound treatment onto a holey carbon film supported on a copper grid. The specimen was air-dried overnight.

Fourier transform infrared (FTIR) spectra of neat PVA film and nanocomposite films were recorded in the attenuated total reflection mode (ATR) using a Nicolet 6700 FTIR Spectrometer (Thermo Scientific) at 2 cm<sup>-1</sup> resolution, in the wavenumber range 500–4000 cm<sup>-1</sup>.

The thermal characteristics of the neat PVA and nanocomposite samples were determined by thermogravimetric analysis (TGA) and differential scanning calorimetry (DSC). The non-isothermal thermogravimetric analysis was realized using a SETSYS Evolution 1750 thermogravimetry analyzer under dynamic argon or air atmospheres at flow rates of 20 and 16 ml min<sup>-1</sup>, respectively. The heating rate in both cases was 10 °C min<sup>-1</sup>. The DSC measurements of the neat PVA and PVA/titania nanocomposites were performed on a DSC 151R SETARAM instrument in the temperature range from 30 to 250 °C. The heating rate was 20 °C min<sup>-1</sup>. The sample weights were in the range 3–3.5 mg for both methods.

## RESULTS AND DISCUSSION

### *Structural characterization of the PVA/TiO<sub>2</sub> nanocomposites*

The shape and size distribution of the TiO<sub>2</sub> nanoparticles used for incorporation into the PVA matrix were estimated by TEM. A TEM image of faceted TiO<sub>2</sub> nanoparticles with an average dimension of about 5 nm is shown in Fig. 1. A selected area electron diffraction pattern (not presented) displayed very broad and diffuse diffraction rings, implying a mainly amorphous structure of the TiO<sub>2</sub> particles. Mainly amorphous structure of the TiO<sub>2</sub> nanoparticles or more precisely the existence of very small crystalline domains was expected due to applied synthetic procedure. Namely, the acidic hydrolysis of titanium tetrachloride occurred at a low temperature (4 °C) and was not accompanied by post-synthetic heating of the obtained colloidal TiO<sub>2</sub> nanoparticles or annealing of the nanoparticles powder. Without additional thermal treatment, the degree of crystallinity of these TiO<sub>2</sub> nanoparticles is very low.

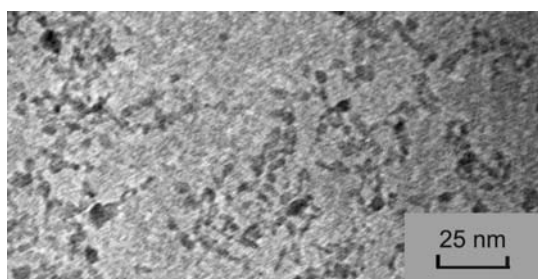
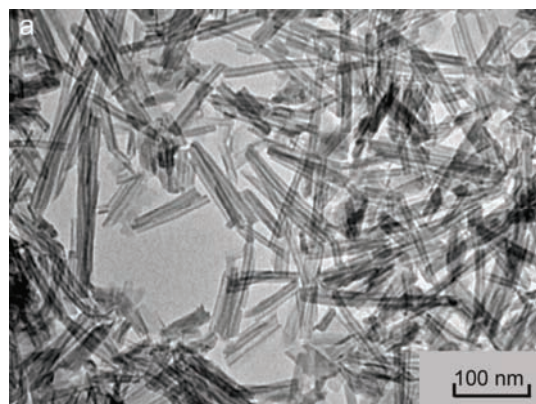


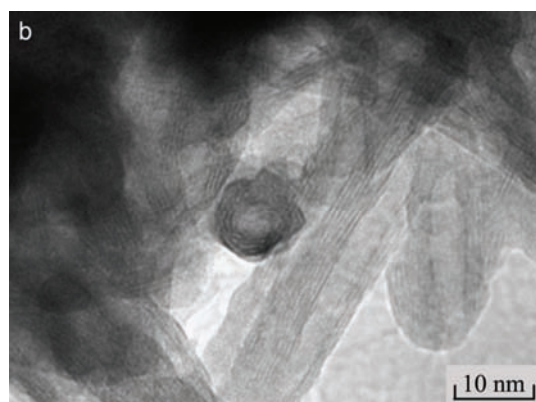
Fig. 1. TEM Image of faceted TiO<sub>2</sub> nanoparticles.

The typical morphology of the titania nanotubes is shown in the Fig. 2a. The conventional TEM image of the same region at a higher magnification, Fig. 2b,

reveals an open-ended multiwall morphology of the scrolled nanotubes. The uniform size distribution of nanotubes outer (approximately 10 nm) and inner (approximately 7 nm) diameters with lengths mainly in the range between 100 and 200 nm was confirmed by conventional TEM measurements. The inter-wall spacing is about 0.73 nm. From the structural point of view, the nanotubes are characterized by quasi-anatase, axially symmetric, distorted octahedral coordination of the Ti atoms with a large fraction of highly reactive five-coordinated sites ( $\approx 40\%$ ) on the surface.<sup>19</sup> These surface sites generally appear as a result of the accommodation of objects in the nanoscale regime for high curvature and surface reconstruction.<sup>19</sup>



(a)



(b)

Fig. 2. TEM Images of tube-like TiO<sub>2</sub> nanoparticles obtained at lower (a) and higher (b) magnification.

A TEM image of the TiO<sub>2</sub> rods is shown in Fig. 3. The presented agglomerate consists of prolate spheroids (rod-like crystallites) with diameters of around 50 nm and lengths in the range from 300 to 700 nm. In a previous study, the anatase crystal form of these rod-like TiO<sub>2</sub> nanoparticles was confirmed, as was

the appearance of spatially confined corner defect (under-coordinated) sites on their tips. The curvature of rods in these regions corresponds to the requested dimension ( $d < 25$  nm).<sup>20</sup>

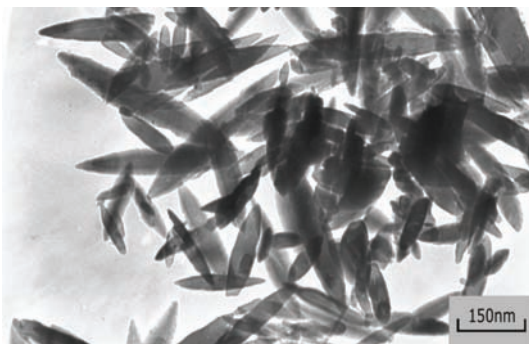


Fig. 3. TEM Image of rod-like  $\text{TiO}_2$  nanoparticles.

The intensity of the interaction between a polymer matrix and similarly shaped nanofillers critically depends on the content and specific surface area of particles, *i.e.*, the inter-particle distance.<sup>21</sup> In order to reveal the possible chemical bonding between the differently shaped  $\text{TiO}_2$  nanoparticles and the PVA matrix, attenuated total reflection Fourier-transform infrared spectrometry was performed over the region 500–4000  $\text{cm}^{-1}$ . The FTIR spectra of the three samples of PVA/ $\text{TiO}_2$  (faceted, rods, tubes) nanocomposite films and the neat PVA film measured in the reflection mode are shown in Fig. 4. All characteristic bands corresponding to PVA can be observed in 500–4000  $\text{cm}^{-1}$  region of the blank PVA film. The symmetric C–C stretching vibration that is an indication of the presence of crystalline regions in PVA is characterized by a band at 1142  $\text{cm}^{-1}$  in each spectrum shown in Fig. 4.<sup>22</sup> The slight decrease in the intensity of this band in the nanocomposite samples compared to the same band in the neat PVA sample confirms a decrease in the crystalline phase of the polymer. The presence of peaks at 1142 and 914  $\text{cm}^{-1}$  in all samples (neat PVA and nanocomposites) reveals the existence of the syndiotactic structure in the polymer chain.<sup>23,24</sup> Taking into account the intensity ratio  $I_{\text{sy}}$  of the peaks at 914 and 830  $\text{cm}^{-1}$  for an evaluation of syndiotacticity level of the PVA, according to Abdelaziz *et al.*<sup>25</sup> and Tawansi *et al.*,<sup>26</sup> a slight decrease was observed only for the PVA/ $\text{TiO}_2$  (tubes) nanocomposite sample. According to Naguro *et al.*,<sup>27</sup> who found a correlation between the increase in the syndiotacticity of PVA and density level of molecular packing in the polymer crystal, it could be assumed that the molecular packing of the PVA/ $\text{TiO}_2$  (tubes) nanocomposite sample was denser, which enables stronger intermolecular hydrogen bonds and lower molecular motions, compared to the other samples with a similar percentage syndiotacticity. A comparison of IR spectra of the PVA matrix and PVA/ $\text{TiO}_2$  nanocomposites revealed changes in the band positioned at 1322  $\text{cm}^{-1}$ . This can be attributed to a coupling of the

O–H plane vibrations (stronger line at 1417 cm<sup>−1</sup>) with C–H wagging vibrations. Therefore, the decrease in the intensity ratio of bands at 1417 and 1322 cm<sup>−1</sup> independently of the shape of TiO<sub>2</sub> nanoparticles implies the existence of a decoupling process between the mentioned vibrations due to interaction between the titania nanoparticles and the OH groups attached to the methane carbons of PVA.<sup>28,29</sup>

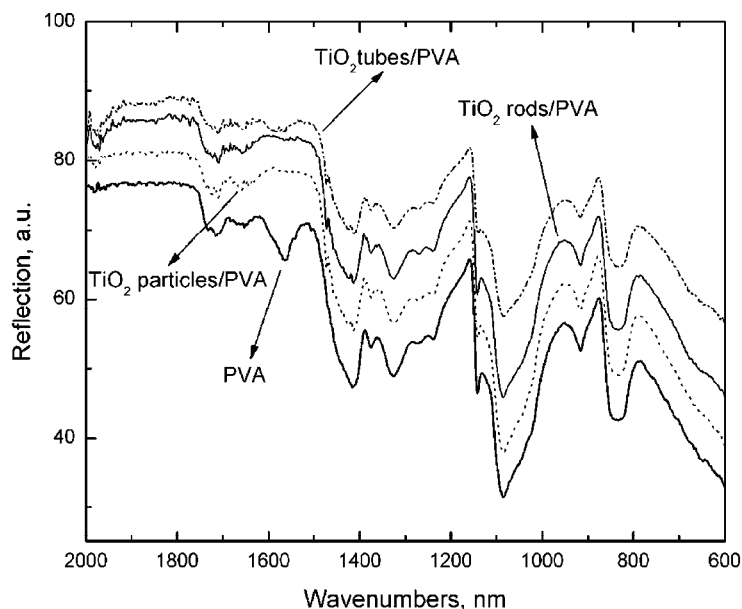


Fig. 4. FTIR Spectra of pure PVA, PVA/TiO<sub>2</sub> faceted particles, PVA/TiO<sub>2</sub> rods and PVA/TiO<sub>2</sub> tubes nanocomposite films.

The most distinct feature in the FTIR spectra of the PVA/TiO<sub>2</sub> nanocomposites was the disappearance of the transmission band at around 1570 cm<sup>−1</sup>, in the spectra of the PVA/TiO<sub>2</sub> particles nanocomposite and the PVA/TiO<sub>2</sub> rods nanocomposite. A remarkable decrease in the intensity of the same band was also observed in the spectrum of the PVA/TiO<sub>2</sub> tubes nanocomposite. According to Krimm *et al.*, PVA may contain some C=O groups within the chain, assigned to  $\beta$ -diketone groups and, consequently, they suggested that the band of this group appears at 1590 cm<sup>−1</sup>.<sup>30</sup> The decision to assign the shifted band at 1570 cm<sup>−1</sup> in neat PVA samples to  $\beta$ -diketone groups, most likely in the enol form, was additionally supported by the presence of band at 1710 cm<sup>−1</sup> associated to the stretching vibration of the C=O functionality.<sup>31</sup> The carbonyl stretching vibration band is verification of the existence of residual vinyl acetate groups in partially hydrolyzed PVA.<sup>32,33</sup> Taking into account the presence of OH groups on the surface of the titania nanocrystals, the possibility of hydrogen bond formation between

them and the  $\beta$ -diketone groups from the polymer chain could be an explanation for the decrease in intensity and disappearance of the band at  $1570\text{ cm}^{-1}$ . The existence of such functionality within PVA chain imparts additional binding locations for  $\text{TiO}_2$  nanoparticles.

#### *Thermal properties of PVA/ $\text{TiO}_2$ nanocomposites*

The influence of the shape, and consequently the different surface areas, of the  $\text{TiO}_2$  nanofillers on the thermal properties of the PVA matrix was examined by non-isothermal TGA and DSC. Their content in the nanocomposites was kept constant. The thermal and thermo-oxidative stability of the PVA/ $\text{TiO}_2$  nanocomposites were compared with the thermal and thermo-oxidative stability of neat PVA. The thermogravimetric (TG) and differential thermogravimetric (DTG) curves obtained under an inert atmosphere for the neat PVA and PVA loaded with differently shaped  $\text{TiO}_2$  nanofillers are shown in Fig. 5. The temperature differences between the neat PVA and PVA/ $\text{TiO}_2$  nanocomposite samples at 50 % weight loss are listed in Fig. 5a.

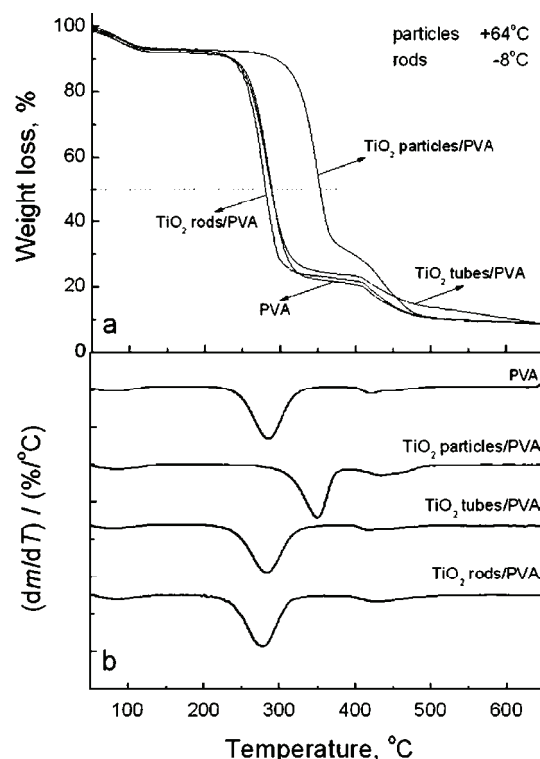


Fig. 5. a) TG and b) DTG curves of pure PVA, PVA/ $\text{TiO}_2$  faceted particles, PVA/ $\text{TiO}_2$  tubes and PVA/ $\text{TiO}_2$  rods nanocomposite samples obtained under an argon atmosphere.

The weight loss that emerges around  $100\text{ }^\circ\text{C}$  is a consequence of loss of physically absorbed moisture and/or evaporation of trapped solvent.<sup>34,35</sup> The

thermal degradation mechanism of the synthesized PVA/TiO<sub>2</sub> nanocomposites and neat PVA in an inert atmosphere mainly consists of two steps initiated by different modes. The first one appears in the range between 250 and 370 °C depending on the shape of particles incorporated into the nanocomposite. The dominant processes during this degradation stage are elimination of OH groups and chain-scission reactions.<sup>36</sup> The major decomposition products are polyenes generated from the dehydration reaction of the PVA chains. Using a highly-hydrolyzed PVA for synthesis of nanocomposite materials, Peng *et al.* confirmed the formation of two polyenes structures, conjugated and non-conjugated, during the first degradation process.<sup>37</sup> During the second degradation step that occurs between 400 and 480 °C depending on the particle shape, chain-scission and Diels–Alder intramolecular and intermolecular cyclization prevailed.<sup>37</sup>

The thermal stability of the PVA/TiO<sub>2</sub> nanocomposites and neat PVA was compared at 50 % weight loss. The presence of shaped TiO<sub>2</sub> nanofillers within the polymer matrix did not affect the degradation mechanism itself, but it demonstrated a noticeable influence on the overall thermal stability of the polymer. The presence of faceted TiO<sub>2</sub> nanoparticles in the nanocomposite caused an increase in the thermal stability of the PVA matrix by 64 °C in an argon atmosphere. Generally, according to the barrier model, it was suggested that the improved thermal stability is due to the formation of polymeric–inorganic char on the surface of the polymer melt, which reduces mass and heat transfer.<sup>38</sup> It can be assumed that the faceted titania nanoparticles inhibited the degradation of the PVA matrix by decreasing the efficiency of OH group elimination and chain-scission reactions. The possible reason for the suppression of these reactions is the interaction of the faceted TiO<sub>2</sub> nanoparticles with the OH groups from the PVA chain. Such interactions may increase the energy barrier for OH group elimination reactions. An additional reason is the reduced mobility of the polymer chains in the presence of the faceted TiO<sub>2</sub> nanoparticles that induces a decrease of their collision frequency and suppresses chain transfer reactions. This type of physical constraint affects the reactions occurring within the second degradation step. It should be emphasized that the considerable increase of PVA thermal stability under a nitrogen atmosphere was achieved with a very low content of TiO<sub>2</sub> nanoparticles (0.25 mass %) in the nanocomposite. In a previous work, the ability of the same type of titania nanoparticles to increase the thermal stability of polystyrene to similar extent under a nitrogen atmosphere was demonstrated but with higher amount of TiO<sub>2</sub> (2 mass %) in the nanocomposite.<sup>39</sup>

The addition of titania nanotubes into the polymer matrix did not have any influence on the thermal stability of the PVA under an inert atmosphere. The decomposition temperature of the PVA matrix (Fig. 5a) slightly decreased by ≈8 °C in the presence of the same amount of titania nanorods. Generally, titania nanotubes and nanorods do not exhibit stabilizing effect on a polymer matrix. It is

well known that polymer adsorption onto surfaces is dominated by a balance between the chain conformational entropy and polymer–substrate interactions.<sup>40</sup> Polymer–substrate interaction favors adsorption in a flat configuration with many contact points and thin layer formation. Titania nanorods and nanotubes separately can be considered as flat surfaces due to their length of a few hundred nanometers and thus, a stabilizing effect on the composite system through the formation of a polymer barrier layer failed. The obtained small decrease in the decomposition temperature of PVA ( $\approx 8$  °C) in the presence of TiO<sub>2</sub> nanorods could be the consequence of increased localized heat conductivity in the nanocomposite sample.

The mechanism of the thermo-oxidative degradation of PVA is more complicated in comparison with that of degradation under an inert atmosphere. Thermo-oxidative degradation process of neat PVA occurs in five stages. The first one appears at around 100 °C and indicates the loss of physically adsorbed water.<sup>41</sup> The partial dehydration of the PVA chains that generates polyene structures occurs in the temperature range between 230 and 300 °C.<sup>42</sup> As a result of the decomposition of polyenes, macroradicals are formed. The polyene macroradicals form *cis*- and *trans*-derivatives. The later form polyconjugated aromatic structures due to intramolecular cyclization and condensation reactions according to the Diels–Alder mechanism in the temperature range between 300 and 400 °C.<sup>42</sup> The fourth degradation step occurring between 400 and 480 °C is a consequence of cyclization and condensation processes of the polyaromatic structures. The final degradation step responsible for the destruction of the carbonized residue occurs between 480 and 600 °C.<sup>42</sup>

The TG and DTG curves of neat PVA and the PVA/TiO<sub>2</sub> nanocomposites obtained under an air atmosphere are shown in Fig. 6.

As in the case under an inert atmosphere, the presence of TiO<sub>2</sub> nanofillers of different shapes in the PVA matrix did not significantly alter the degradation mechanism, but did affect the overall thermal stability. The evidenced noticeable overall increase in the thermal stability of the PVA matrix in the presence of the faceted nanoparticles is the consequence of increased temperatures of the following processes: generation of polyene structures ( $\Delta T \approx 44$  °C), formation of polyconjugated aromatic structures ( $\Delta T \approx 57$  °C), cyclization and the condensation of polyaromatic structures ( $\Delta T \approx 9$  °C) and the destruction of carbonized residues ( $\Delta T \approx 8$  °C).

The thermo-oxidative stability of the PVA matrix was more influenced by the presence of titania nanotubes and nanorods than its thermal stability in an inert atmosphere. According to the curves presented in Fig. 6b, it could be concluded that the presence of the nanotubes had inhibitory effects on the cyclization processes and on the condensation of polyaromatic structures ( $\Delta T \approx 28$  °C) and destruction of the carbonized residues ( $\Delta T \approx 53$  °C). In the sample of PVA/TiO<sub>2</sub>

rods nanocomposite, only the final degradation step of the PVA matrix, the destruction of the carbonized residue, was shifted toward higher temperature by  $\approx 25$  °C compared to that of the neat PVA sample.

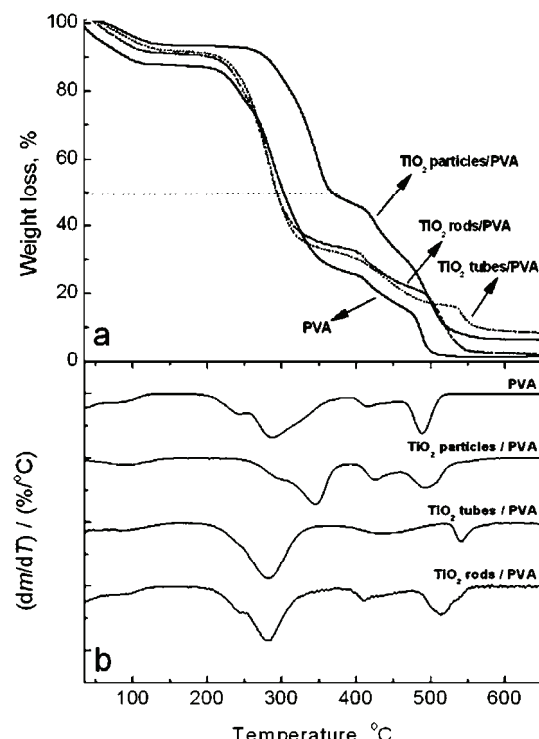


Fig. 6. a) TG and b) DTG curves of pure PVA, PVA/TiO<sub>2</sub> faceted particles, PVA/TiO<sub>2</sub> tubes and PVA/TiO<sub>2</sub> rods nanocomposite samples obtained under an air atmosphere.

Residues at 600 °C under both atmospheres (inert and air) were detected. It could be observed (Figs. 5a and 6a) that the residue in an inert atmosphere was larger than in an air atmosphere. Thomas *et al.* suggested that the large residue in an inert atmosphere could be expected since the pyrolyzation results in the formation of amorphous carbon.<sup>43</sup> The residue observed in an air atmosphere is a consequence of the effects of geometry on the degradation process.

PVA is a semi-crystalline polymer with a decomposition temperature close to its melting temperature.<sup>6</sup> This fact complicates conclusions on the perfection of its crystallinity based on melting temperature measurements.

The DSC curves of the synthesized PVA/TiO<sub>2</sub> nanocomposites and of the corresponding neat PVA obtained during heating are shown in Fig. 7a. Two endothermic peaks in all samples are evident. The broad signals in the temperature range from 60 to 100 °C arose due to vaporization of physically adsorbed water.<sup>44,45</sup> The peak that appears between 200 and 250 °C in the curves of the samples corresponds to the melting temperature ( $T_m$ ). It should be stressed that

the melting temperature of the polymer matrix was not affected by the addition of the faceted  $\text{TiO}_2$  nanoparticles, indicating a lack of their influence on the heat resistance in an inert atmosphere. The presence of titania nanotubes or titania nanorods in the PVA matrix slightly increased the melting temperature of the polymer by  $\approx 2$  and  $\approx 3$  °C, respectively. Such small rises in the melting temperature of the PVA/ $\text{TiO}_2$  tubes and PVA/ $\text{TiO}_2$  rods nanocomposites are likely due to a modification in the diffusion of volatiles in the polymer or simply to a different tortuosity of polymer chains depending on the particle shape.

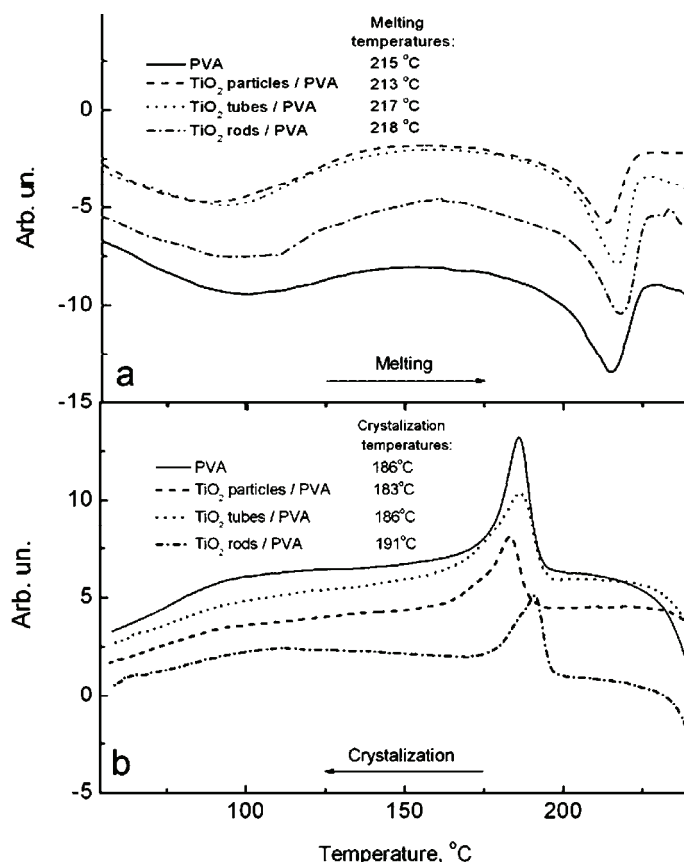


Fig. 7. DSC Curves of pure PVA, PVA/ $\text{TiO}_2$  nanoparticles, PVA/ $\text{TiO}_2$  tubes and PVA/ $\text{TiO}_2$  rods nanocomposite samples obtained under a nitrogen atmosphere in a) heating and b) cooling processes.

The DSC thermograms of the synthesized PVA/ $\text{TiO}_2$  nanocomposites and the neat PVA polymer obtained in cooling process are shown in Fig. 7b. It is clear that the titania nanorods induced the nucleation of the PVA matrix at an earlier stage, *i.e.*, at a higher temperature, during the cooling run, compared to the

neat PVA. The OH groups existing on the particle surface may act as nucleation sites together with the adequate morphology of the nanoparticles.<sup>6,46</sup>

The geometry of the faceted TiO<sub>2</sub> nanoparticles present in the PVA matrix caused a slight delay of the onset of crystallization and, consequently, decreased the crystallization temperature of the nanocomposite ( $T_c = 183$  °C). The presence of titania nanotubes did not affect the crystallization process at all ( $T_c = 186$  °C).

The degree of crystallinity ( $X_c$ ) of PVA in the presence of the shaped TiO<sub>2</sub> nanoparticles was calculated using the following equation:

$$X_c (\%) = 100(\Delta H_c/(1-f)\Delta H_m)$$

where  $\Delta H_m$  is the enthalpy corresponding to the melting of a 100 % crystalline sample (138.6 J g<sup>-1</sup>),<sup>47</sup>  $\Delta H_c$  is the apparent enthalpy of crystallization corresponding to the nanocomposite sample and  $f$  is the weight fraction of TiO<sub>2</sub> nanoparticles in the PVA/TiO<sub>2</sub> nanocomposite.

The incorporation of faceted TiO<sub>2</sub> nanoparticles into the PVA matrix led to a slight decrease in the degree of crystallinity of PVA ( $X_c = 32$  %) compared to neat PVA ( $X_c = 38$  %) despite the excess of OH groups on the particles surface that may act as nucleation sites. The decrease in crystallinity, as well as the delay of the onset of crystallization, is likely caused by a reduction of the PVA chain mobility and by possible hydrogen bonding formation between the surface OH groups of the faceted TiO<sub>2</sub> nanoparticles and the PVA chain. According to DSC measurements, titania nanorods and nanotubes did not affect the degree of crystallinity of PVA in PVA/TiO<sub>2</sub> rods ( $X_c = 39$  %) and PVA/TiO<sub>2</sub> tubes ( $X_c = 38$  %) nanocomposites.

In general, the first step of any crystallization process is nucleation. When the critical size is attained, these nuclei become the centers for the growth of polymer crystalline phase. The overall crystallization rate is attributed to the contribution of both nucleation and growth rates. The rate of nucleation is higher as the temperature drops. The determining factor is the degree of supercooling  $T_m - T_c$ , which presents the difference between the melting point  $T_m$  and the temperature of crystallization  $T_c$  (crystallization at temperatures  $T_c$  below the melting point  $T_m$ ).<sup>48</sup> The rate of crystal growth is mainly determined by the mobility of the polymer chains in the melt. Therefore, according to Ou *et al.*<sup>49</sup> and Krijgsman *et al.*,<sup>50</sup> the degree of supercooling is an indication of polymer crystallizability during a non-isothermal process. In other words the smaller the difference, ( $T_m - T_c$ ), the higher the overall crystallization rate.

Analyzing the  $T_m - T_c$  values for all the investigated samples, it could be noticed that incorporation of the shaped TiO<sub>2</sub> nanofillers into the PVA matrix did not significantly change the overall crystallization rate of the polymer. Such conclusion is based on the small differences in the degree of supercooling between the neat PVA ( $T_m - T_c = 29$  °C) and PVA/TiO<sub>2</sub> particles ( $T_m - T_c = 30$  °C), PVA/

/TiO<sub>2</sub> tubes ( $T_m - T_c = 31$  °C) and PVA/TiO<sub>2</sub> rods ( $T_m - T_c = 27$  °C) nanocomposites. According to obtained values of the  $T_c/T_m$  ratio, in the range from 0.86 to 0.88 for all samples, and the Mandelkern rule, the rates of crystallization processes in the PVA-based nanocomposites are relatively high.<sup>51</sup>

### CONCLUSIONS

Three PVA/TiO<sub>2</sub> nanocomposite samples were synthesized by direct blending of PVA and differently shaped TiO<sub>2</sub> nanofillers (faceted nanoparticles, nanotubes or nanorods) as precursors. The interaction between PVA polymer chains and the surface of the titania nanofillers was confirmed by FTIR spectroscopy in the reflection mode. It was found that the same amount of TiO<sub>2</sub> nanofillers independent of the shape did not change the degradation mechanism of PVA in argon and air atmospheres. The faceted nanoparticles ( $d \approx 5$  nm) increased the thermal stability of the PVA matrix by 64 °C under an inert atmosphere. The presence of TiO<sub>2</sub> nanotubes ( $d = 10$  nm,  $L < 200$  nm) and titania nanorods ( $d \approx 50$  nm,  $300 < L < 700$  nm) did not exhibit a stabilizing effect on the thermal properties of the polymer matrix under an argon atmosphere. The temperature of the thermo-oxidative degradation of PVA increased with addition of faceted TiO<sub>2</sub> nanoparticles. The presence of titania nanotubes had inhibitory effect only on the cyclization reactions and the condensation of the polyaromatic structure and destruction of the carbonized residues, which appeared at higher temperatures during the thermo-oxidative degradation of the PVA matrix. In the course of cooling, titania nanorods induced crystallization of PVA at a higher temperature. The degree of crystallinity of the polymer matrix in the presence of faceted TiO<sub>2</sub> nanoparticles decreased ( $X_c = 32\%$ ) compared with the degree of crystallinity of the neat PVA ( $X_c = 38\%$ ).

*Acknowledgements.* Financial support for this study was granted by the Ministry of Education and Science of the Republic of Serbia under Projects 172056 and 45020.

### ИЗВОД

#### УТИЦАЈ ОБЛИКА ТИТАН-ДИОКСИДНИХ НАНОПУНИЛАЦА НА ТЕРМАЛНЕ КАРАКТЕРИСТИКЕ ПОЛИВИНИЛ-АЛКОХОЛА

МАРИЈА Б. РАДОИЋИЋ<sup>1</sup>, ЗОРАН В. ШАПОЊИЋ<sup>1</sup>, МИЛЕНА Т. МАРИНОВИЋ-ЦИНЦОВИЋ<sup>1</sup>,  
SCOTT P. AHRENKIEL<sup>2</sup>, НАТАША М. БИБИЋ<sup>1</sup> И ЈОВАН М. НЕДЕЉКОВИЋ<sup>1</sup>

<sup>1</sup>Институција за нуклеарне науке Винча, Ј. Џр. 522, 11001 Београд и <sup>2</sup>South Dakota School of Mines and Technology, Rapid City, SD, USA

Нанокомпозити на бази поливинил-алкохола (PVA) и TiO<sub>2</sub> нанокристала различитих облика и величина (наночестице, нанотубе и наноштапићи) синтетисани су методом директног мешања раствореног полимера (1,5 mas. %) и колоидних раствора/прахова нанокристала TiO<sub>2</sub> (0,25 mas. %). У циљу испитивања утицаја облика титан-диоксидних нанокристала на њихову интеракцију са PVA ланцима и термалну стабилност полимерне матрице, урађена је структурна и термална карактеризација PVA/TiO<sub>2</sub> нанокомпозита. Уочено је да иста коли-



чина TiO<sub>2</sub> нанокристала, независно од њиховог облика, не утиче на механизам деградације PVA како на ваздуху тако ни у атмосфери аргона. Наночестице TiO<sub>2</sub> ( $d \approx 5$  nm) повећавају термалну стабилност PVA матрице за 64 °C, док титан-диоксидне нанотубе ( $d = 10$  nm,  $L < 200$  nm) и наноштапићи ( $d \approx 50$  nm,  $300 < L < 700$  nm) не показују стабилизациони утицај на полимерну матрицу у атмосфери аргона. Термо-оксидативна стабилност PVA расте са додатком TiO<sub>2</sub> наночестица. Приликом хлађења PVA/TiO<sub>2</sub> нанокомпозита, TiO<sub>2</sub> наноштапићи индукују кристализацију PVA на вишим температурама. Степен кристалиничности PVA матрице је благо умањен у присуству наночестица TiO<sub>2</sub> у нанокомпозитном узорку ( $X_c = 32\%$ ) у поређењу са степеном кристалиничности чистог PVA ( $X_c = 38\%$ ).

(Примљено 31. марта, ревидирано 29. јуна 2011)

#### REFERENCES

1. W. Caseri, *Macromol. Rapid Commun.* **21** (2000) 705
2. D. Y. Godovsky, *Adv. Polym. Sci.* **153** (2000) 163
3. E. Džunuzović, M. Marinović-Cincović, K. Jeremić, J. Vuković, J. Nedeljković, *Polym. Degrad. Stab.* **93** (2008) 77
4. J. Zheng, R. Ozisik, R. W. Siegel, *Polymer* **46** (2005) 10873
5. J. K. Pandey, K. R. Reddy, A. P. Kumar, R. P. Singh, *Polym. Degrad. Stab.* **88** (2005) 234
6. Z. Peng, D. Chen, *J. Polym. Sci., B* **44** (2006) 534
7. K. Yamamura, N. Kuranuki, M. Suzuki, T. Tanigami, S. Matsuzawa, *J. Appl. Polym. Sci.* **41** (1990) 2409
8. Y. Li, K. G. Neoh, E. T. Kan, *Polymer* **45** (2004) 8779
9. J. Kuljanin, M. I. Čomor, V. Djoković, J. M. Nedeljković, *Mater. Chem. Phys.* **95** (2006) 67
10. L. Liu, Z. Qi, X. Zhu, *J. Appl. Polym. Sci.* **71** (1999) 1133
11. J. Kuljanin-Jakovljević, Z. Stojanović, J. M. Nedeljković, *J. Mater. Sci.* **41** (2006) 5014
12. H. Gerischer, A. Heller, *J. Phys. Chem.* **95** (1991) 5261
13. G. J. Meyer, *J. Chem. Edu.* **74** (1997) 652
14. L. X. Chen, T. Rajh, Z. Wang, M. C. Thurnauer, *J. Phys. Chem., B* **101** (1997) 10688
15. T. Rajh, A. E. Ostafin, O. I. Mićić, D. M. Tiede, M. C. Thurnauer, *J. Phys. Chem.* **100** (1996) 4538
16. R. C. Thompson, *Inorg. Chem.* **23** (1984) 1794
17. T. Kasuga, M. Hiramatsu, A. Hoson, T. Sekino, K. Niihara, *Adv. Mater.* **11** (1999) 1307
18. N. M. Dimitrijević, Z. Šaponjić, B. M. Rabatic, O. G. Poluektov, T. Rajh, *J. Phys. Chem., C* **111** (2007) 14597
19. Z. Šaponjić, N. Dimitrijević, D. Tiede, A. Goshe, X. Zuo, L. Chen, A. Barnard, P. Zapol, L. Curtiss, T. Rajh, *Adv. Mater.* **17** (2005) 966
20. B. Rabatic, N. Dimitrijević, R. Cook, Z. Šaponjić, T. Rajh, *Adv. Mater.* **18** (2006) 1033
21. D. Šajinović, Z. Šaponjić, N. Cvjetičanin, M. Marinović-Cincović, J. Nedeljković, *Chem. Phys. Lett.* **329** (2000) 168
22. S. K. Mallapragada, N. A. Peppas, *J. Polym. Sci., B* **34** (1996) 1339
23. S. Rajendran, M. Sivakumar, R. Subadevi, *Mater. Lett.* **58** (2004) 641
24. S. Murahashi, H. Yûcki, T. Sano, U. Yonemura, H. Tadokoro, Y. Chatani, *J. Polym. Sci.* **62** (1962) 77
25. M. Abdelaziz, *J. Appl. Polym. Sci.* **94** (2004) 2178



26. A. Tawansi, H. M. Zidan, A. H. Oraby, M. E. Dorgham, *J. Phys., D* **31** (1998) 3428
27. M. Nagura, S. Matsuzawa, K. Yamaura, H. Ishikawa, *Polym. J.* **14** (1982) 69
28. Z. H. Mbhele, M. G. Salemane, C. G. van Sittert, J. M. Nedeljković, V. Djoković, A. S. Luyt, *Chem. Mater.* **15** (2003) 5019
29. B. Karthikeyan, *Physica B* **364** (2005) 328
30. S. Krimm, C. Y. Liang, G. B. B. M. Sutherland, *J. Polym. Sci.* **22** (1956) 227
31. G. Socrates, *Infrared and Raman characteristic group frequencies: Tables and Charts*, Wiley, New York, 2001 p. 115
32. S. M. Rabie, N. Abdel-Hakeem, M. A. Moharram, *J. Appl. Polym. Sci.* **38** (1989) 2269
33. P. Alexy, D. Kachova, M. Krsiak, D. Bakos, B. Simkova, *Polym. Degrad. Stab.* **78** (2002) 413
34. C. C. Yang, S. J. Chiu, K. T. Lee, W. C. Chien, C. T. Lin, C. A. Huang, *J. Power Sources* **184** (2008) 44
35. D. Lopez, I. Cendoya, F. Torres, J. Tejada, C. Mijangos, *J. Appl. Polym. Sci.* **82** (2001) 3215
36. J. W. Gilman, D. L. Vander Hart, T. Kashiwagi, *ACS Symp. Ser.* **599** (1994) 161
37. Z. Peng, L. X. Kong, *Polym. Degrad. Stab.* **92** (2007) 1061
38. A. N. Krklješ, M. T. Marinović-Cincović, Z. M. Kačarević-Popović, J. M. Nedeljković, *Thermochim. Acta* **460** (2007) 28
39. E. Džunuzović, V. Vodnik, K. Jeremić, J. M. Nedeljković, *Mater. Lett.* **63** (2009) 908
40. E. Tadd, A. Zeno, M. Zubris, N. Dan, R. Tannenbaum, *Macromolecules* **36** (2003) 6497
41. P. Budrigeac, *J. Therm. Anal. Cal.* **92** (2008) 291
42. A. Y. Shaulov, S. M. Lomakin, T. S. Zarkhina, A. D. Rakhimkulov, N. G. Shilkina, Y. B. Muravlev, A. A. Berlin, *Dokl. Phys. Chem.* **403** (2005) 154
43. P. S. Thomas, J. P. Guerbois, G. F. Russell, B. J. Briscoe, *J. Therm. Anal. Cal.* **64** (2001) 501
44. Q. Wu, J. Zhang, S. Sang, *J. Phys. Chem. Solids* **69** (2008) 2691
45. A. N. Krklješ, M. Marinović-Cincović, Z. Kačarević-Popović, J. M. Nedeljković, *Eur. Polym. J.* **43** (2007) 2171
46. W. B. Xu, P. S. He, *Polym. Eng. Sci.* **41** (2001) 1903
47. Z. Peng, L. X. Kong, S. D. Li, *Polymer* **46** (2005) 1949
48. A. Ram, *Fundamentals of polymer engineering*, Plenum Press, New York, 1997, p. 51
49. C. F. Ou, M. T. Ho, J. R. Lin, *J. Polym. Res.* **10** (2003) 127
50. J. Krijgsman, G. J. E. Biemond, R. J. Gaymans, *J. Appl. Polym. Sci.* **103** (2007) 512
51. M. M. Feldstein, G. A. Shandryuk, S. A. Kuptsov, N. A. Plate, *Polymer* **41** (2000) 5327.

